Journal of Advanced Ceramics
2012, 1(4): 268-273
DOI: 10.1007/s40145-012-0034-9 ISSN 2226-4108

Research Article

Crystal structure determination of nanolaminated $Ti_5Al_2C_3$ by combined techniques of XRPD, TEM and *ab initio* calculations

Hui ZHANG[a,b], Xiaohui WANG[a], Yonghui MA[a], Luchao SUN[a,b], Liya ZHENG[a,b], Yanchun ZHOU[c,*]

[a]*Shenyang National Laboratory for Materials Science*, *Institute of Metal Research*, *Chinese Academy of Sciences*, *72 Wenhua Road*, *Shenyang 110016*, *China*
[b]*Graduate School of Chinese Academy of Sciences*, *Beijing 100039*, *China*
[c]*Science and Technology on Advanced Functional Composite Laboratory*, *Aerospace Research Institute of Materials & Processing Technology*, *No.1 South Dahongmen Road*, *Beijing 100076*, *China*

Received: November 23, 2012; Accepted: November 27, 2012

Abstract: Crystal structure of $Ti_5Al_2C_3$ was determined by means of X-ray powder diffraction (XRPD), transmission electron microscopy (TEM) and *ab initio* calculations. In contrast to the already known $P6_3/mmc$ space group that the MAX phases crystallize, it was demonstrated that the $R\bar{3}m$ space group could better satisfy the experimental data. The lattice parameters are $a = 0.305\,64$ nm, $c = 4.818\,46$ nm in a hexagonal unit cell.

Key words: $Ti_5Al_2C_3$; crystal structure; layered carbides; transmission electron microscopy (TEM)

1 Introduction

Ti_2AlC and Ti_3AlC_2 are the most light-weight and oxidation resistant nanolaminated ternary carbides with a general formula $Ti_{n+1}AlC_n$ ($n = 1, 2$) in the Ti-Al-C system [1]. These two carbides belong to the $M_{n+1}AX_n$ phases [2], referred as MAX phases (where M is an early transition metal, A is an A group element, X is C and/or N, and $n = 1, 2, \cdots$). According to the value of n, these compounds are also called 211, 312, 413 phases and so on [1-3]. Up to now, there are over 60 MAX phases have been identified. Due to the unique nanolaminated crystal structure and anisotropic bonding nature, Ti_2AlC and Ti_3AlC_2, as the representatives of the MAX phases, exhibit the merits of both metals and ceramics [1,2]. Like metals, they are readily machinable, resistant to thermal shock, thermally and electrically conductive and damage tolerant. Like ceramics, they are refractory, elastically stiff, and resistant to oxidation and chemical attack. The excellent properties of the MAX phases ignited a worldwide research enthusiasm. Recently, some new nanolaminated carbides including $Ti_5Si_2C_3$ (523 phase) [4], $Ti_5Ge_2C_3$ [5], $Ti_5Al_2C_3$ [6], $(V, Cr)_5Al_2C_3$ [7] that cannot be described by the $M_{n+1}AX_n$ formula, were microscopically observed. These newly identified nanolaminated carbides together with the already known MAX phases follow a general formula $M_nA_mX_{n-m}$ ($n \geqslant 2m$, n and m are integers). They are

* Corresponding author.
E-mail: yczhou714@gmail.com

still called MAX phases.

Prior to the submission of the present paper, the nanolaminated MAX phases exclusively crystallize in a hexagonal structure with the space group of $P6_3/mmc$. Wilhelmsson *et al*. [6] observed a stacking sequence corresponding to $Ti_5Al_2C_3$ in the Ti_3AlC_2 film deposited at 900 ℃. Zhou *et al*. [7] observed a similar stacking sequence corresponding to $(V, Cr)_5Al_2C_3$ in bulk $(V, Cr)_2AlC$ samples. They suggested that the unit cell of these 523 phases can be described as halves of unit cells of 211 and 312, which was regarded as an intergrown structure [3,6]. Recently, Wang *et al*. [8] identified $Ti_5Al_2C_3$ in a bulk sample as a new nanolaminated MAX phase in the Ti-Al-C system. The stacking sequence of $Ti_5Al_2C_3$ could be described as alternate stacking of Ti-C-Ti and Ti-C-Ti-C-Ti layers between each Al layer. Palmquist *et al*. [4] synthesized $Ti_5Si_2C_3$ in thin films, and pointed out that the symmetry of the hexagonal space group D_{6h}^4 is broken due to the three repetition of alternating two and three Ti layers [4]. Our previous work demonstrated that the crystal structure of $Ti_5Al_2C_3$ can be constructed with the space group D_{6h}^4, allowing the edge sharing Ti_6C octahedrons a slight distortion [8]. Very recently, Lane *et al*. [9] reported another method to produce $Ti_5Al_2C_3$ by topotactic transformation from Ti_2AlC and a crystal structure with the $P3m1$ space group was proposed [10]. The controversy on the crystal structure of a new compound is very common. For example, $ZrAlC_{1-x}$ was first reported by Michalenko *et al*. [11] in 1979 and it was identified to crystallize in hexagonal symmetry with a space group of $P6_3/mmc$. In 1980, Schuster and Nowotny [12] discovered a new $Zr_2Al_3C_{5-x}$ phase that crystallized with a space group of P31c. Parthé and Chabot [13] investigated the crystal structure of $Zr_2Al_3C_{5-x}$ phase and determined its symmetry as $P6_3/mmc$. By considering C occupation in Zr_6C octahedrons, they also stated that the real composition of $Zr_2Al_3C_{5-x}$ should be $Zr_2Al_3C_4$. Gesing and Jeitschko [14] re-examined the composition and crystal structure of $ZrAlC_{1-x}$ using X-ray diffraction (XRD) technique and the space group was determined as $P6_3/mc$ and the composition was identified as $Zr_3Al_3C_5$. Lin *et al*. [15] using a combinational techniques of selected area electron diffraction (SAED) and convergent beam electron diffraction (CBED), determined the space group of both $Zr_2Al_3C_4$ and $Zr_3Al_3C_5$ as $P6_3/mmc$. Similarly, more intensive studies are needed to understand the crystal structure of $Ti_5Al_2C_3$, a new phase with complex structure in the Ti-Al-C system.

In this study, closer structural examinations of $Ti_5Al_2C_3$ by electron diffraction demonstrate that most of the grains corresponding to the composition of $Ti_5Al_2C_3$ crystallize in the $R\bar{3}m$ space group. *Ab initio* calculations indicate that the structure with the $P6_3/mmc$ space group is less stable at ground state, and less consistent with the experimental data. Adopting the $R\bar{3}m$ space group could better satisfy the experimental X-ray powder diffraction (XRPD) data in Rietveld refinement.

2 Experimental procedure

The bulk sample used in the present work was prepared by the method that has been reported before [8,16,17] and not shown here for brevity. Powders were drilled and examined in an X-ray diffractometer (Rigaku D/max-2400, Tokyo, Japan) with Cu$K\alpha$ radiation. Microstructure characterization using high resolution transmission electron microscopy (HRTEM) was conducted in a Tecnai G^2 F20 analytic transmission electron microscope working at 200 kV. SAED and CBED patterns were taken in a JEOL2100 by tilting the required zone-axis exactly along the beam direction. SAED and CBED patterns are enhanced for the purpose of clear visibility of the weak details. Calculated XRPD patterns and structural parameters were obtained by Rietveld refinement using DBWS code in Cerius^2 computation program for material research (Molecular Simulation Inc., San Diego, CA). Geometry optimization was completed by *ab initio* calculations using the CASTEP code [18]. The basis set cutoff and the Brillion zone sampling were 450 eV and 10×10×2 special *k*-point meshes [19], respectively. Interaction of electrons with ion cores was represented by the Vanderbilt-type ultrasoft pseudopotential [20]. The electronic exchange-correlation energy was treated under GGA-PW91 [21]. The BFGS minimization method was used in geometry optimization [22], and the tolerances were selected as the difference in total energy within 5×10^{-5} eV/atom, maximum ionic Hellmann-Feynman force within 0.01 eV/Å, maximum ionic displacement within 5×10^{-4} Å, and maximum stress within 0.02 GPa.

3 Results and Discussion

Figure 1 shows the XRPD pattern of the as-synthesized sample. The relatively weak, unindexed peaks belong to $Ti_5Al_2C_3$, according to the work of Wang *et al.* [8]. The peak of the highest intensity overlaps with those of Ti_3AlC_2 and Ti_2AlC at $2\theta = 39.5°$. Figure 2 shows a low-magnification TEM bight field image of $Ti_5Al_2C_3$. Like other already known MAX phases, the grains crystallize in the form of thin slabs.

To intensively inspect the structure of $Ti_5Al_2C_3$, SAED and tilt experiments were conducted. Figures 3(a) to 3(c) present the electron diffraction patterns (EDPs) of $Ti_5Al_2C_3$. An EDP, as shown in Fig. 3(c), was obtained when the thin-film specimen was tilted by 30° from the direction of the zone-axis of the EDP in Fig. 3(b). An interesting phenomenon is that the angle between $\mathbf{R}_2$ and $\mathbf{R}_1$ is 96.2°, and the angle between $\mathbf{R}_3$ and $\mathbf{R}_1$ is 93.2°, as shown in Fig. 3(b). This result is different from the right angle in the EDP collected along the $[11\bar{2}0]$ zone-axis when $Ti_5Al_2C_3$ is assigned to the $P6_3/mmc$ space group. The slight difference suggests that the investigated $Ti_5Al_2C_3$ grains might not belong to the $P6_3/mmc$ space group. Meanwhile, all the obtained EDPs belonging to low-index axes could be indexed based on a hexagonal cell, belonging to trigonal crystal system, as shown in Figs. 3(a) to 3(c). It is worth noting that the $(0003n)$ reflections may be caused by double diffraction effect with the reflection condition $(0006n)$ in a crystal belonging to the $R3c$ or $R\bar{3}c$ space group, where the $h\bar{h}0l$ reflections appear only when l is even and $l + h = 3n$. But this possibility could be ruled out by the following two facts: (1) there is a weak peak at $2\theta = 5.33°$ corresponding to (0003), as shown in the inset of Fig. 1; (2) the diffraction spot corresponding to $(\bar{1}101)$ appears when the electron incident beam is parallel to $[11\bar{2}0]$, as shown in Fig. 3(b). Thus, the reflection conditions are summarized as follows: $hki0$:

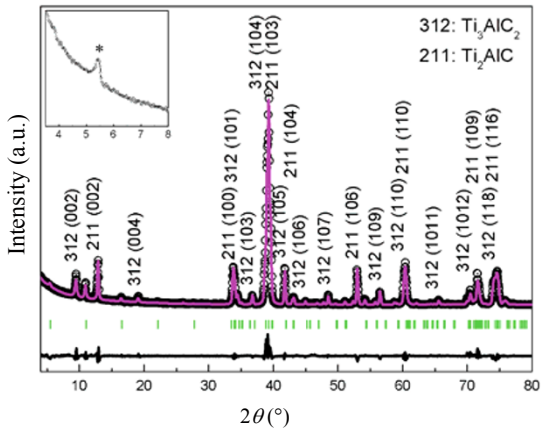

Fig. 1 Comparison between experimental and calculated XRPD patterns of $Ti_5Al_2C_3$. Inset presents the 2θ range from 3.5° to 8°, showing the (0003) reflection.

Fig. 2 Low-magnification TEM bright field image of $Ti_5Al_2C_3$.

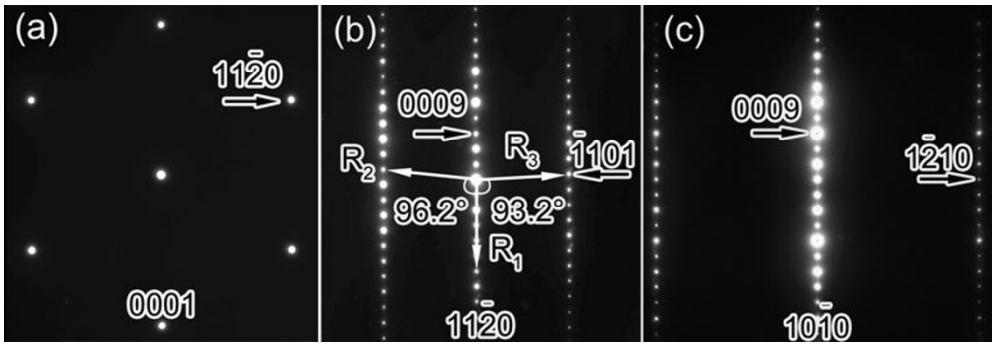

Fig. 3 (a)-(c) EDPs of $Ti_5Al_2C_3$, which are indexed as $[0001]$, $[11\bar{2}0]$, $[10\bar{1}0]$, respectively, shown at the bottom of each pattern.

$h-k=3n$; $h\bar{h}0l$: $l+h=3n$; $h\bar{2}\bar{h}hl$: $l=3n$; $000l$: $l=3n$. According to these reflecting conditions, the possible space groups of $Ti_5Al_2C_3$ investigated in this study are: $R3$, $R\bar{3}$, $R32$, $R3m$, $R\bar{3}m$.

It is well acknowledged that the symmetry of a crystal can be directly observed through the strong dynamical diffraction effects using CBED [23]. Thus the CBED technique is a powerful tool to determine the space group of an unknown phase [23,24]. To uniquely determine the space group of $Ti_5Al_2C_3$, zone-axis patterns were recorded at various camera lengths and different convergence semiangles, as presented in Fig. 4. Figs. 4(a), 4(c) and 4(d) show whole patterns (WPs) recorded at different convergence semiangles and camera lengths with the beam aligned along [0001], both show a symmetry of three-fold rotation axis and 3 mirrors related by the rotation axis. The existing of mirrors is highlighted in Fig. 4(b), which was recorded when the sample was tilted slightly away from the [0001] along g = $10\bar{1}0$. The symmetry of the WPs is $3m$. Fig. 4(e) shows a bright pattern corresponding to [0001], and also shows symmetry of $3m$. The corresponding diffraction group is $3m$ or 6_Rmm_R, and the point group is $3m$ or $\bar{3}m$ [23], considering the indexing results of the EDPs belonging to the low-index zone axes. Fig. 4(f) shows a WP belonging to [$11\bar{2}0$]. It is obviously demonstrated that there is an axis of two-fold rotation along [$11\bar{2}0$]. Since the diffraction group of $3m$ and $\bar{3}m$ along [$11\bar{2}0$] is 1_R and 21_R [23], respectively, the point group of $Ti_5Al_2C_3$ investigated in this study is $\bar{3}m$, and the space group is $R\bar{3}m$(166).

In the MAX phases, the slightly distorted M_6X octahedrons are edge-sharing [2]. Raman spectrum, not shown here, indicates that the Ti-C bonding of $Ti_5Al_2C_3$ also shares this feature, and the value of fractional x and y of the atoms' site in the hexagonal unit cell should be 1/3 or 2/3 or 0 for $Ti_5Al_2C_3$. The HRTEM image of $Ti_5Al_2C_3$, shown in Fig. 5(a), indicates that the distance between Ti layer and Al layer is about 2.5 Å and that between Ti layer and C layer is about 1.05 Å. According to the EDPs in Fig. 3, a is roughly 3.02 Å, and c is about 48.47 Å, namely $18d_{Ti\text{-}C}+12d_{Al\text{-}Ti}$ (48.9 Å). Referring to the HRTEM image, an initial structure is constructed. The parameters for this structure are summarized in Table 1. A unit cell contains 3 times the formula, namely the cell formula is $Ti_{15}Al_6C_9$. For the sake of further

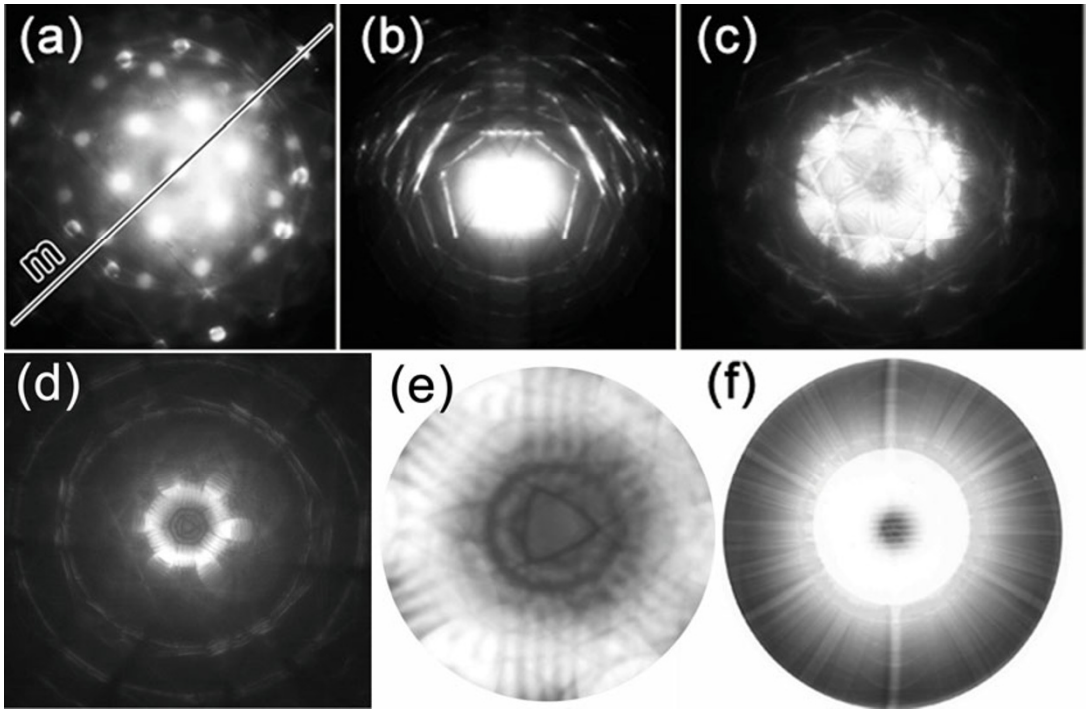

Fig. 4 (a) CBED pattern taken along [0001]; (b) CBED pattern recorded when the sample was tilted away from [0001] along $\boldsymbol{g}$ = $10\bar{1}0$; (c)-(e) CBED patterns taken with different camera lengths and convergence semiangles; (f) CBED pattern taken at [$11\bar{2}0$] incidence, shows the symmetry of two-fold rotation axis.

determination of structure parameters, the initial structure was refined by Rietveld method. The refined structure parameters are included in Table 2. The calculated XRD pattern and the difference curve are shown in Fig. 1. The reliability factors are $R_p = 7.86\%$, $R_{wp} = 11.06\%$, respectively. The phase composition was determined to be 19.7 mass% $Ti_5Al_2C_3$, 34.5 mass% Ti_3AlC_2, and 45.8 mass% Ti_2AlC. For comparison, the structure parameters determined by geometry optimization using CASTEP code are also listed in Table 2. It can be seen that the experimental data agree well with the theoretical ones. The projection on the plane of $(11\bar{2}0)$, simulated using the equilibrium crystal structure, is depicted in Fig. 5(b), which agrees well with the HRTEM image shown in Fig. 5(a).

Palmquist *et al.* [4] observed $Ti_5Si_2C_3$ in deposited Ti-Si-C films. To the best knowledge of the authors, there is no report on the successful synthesis of bulk sample of single 523 phase. It is likely that the 523 phases are metastable, especially for $Ti_5Al_2C_3$ [4,6]. In the present work, the mass percent of $Ti_5Al_2C_3$ in the as-synthesized bulk sample is over 19%, indicating that the $Ti_5Al_2C_3$ is stable at 1580 ℃.

Table 1 Structure parameters used to construct the initial unit cell of $Ti_5Al_2C_3$

Formula			$Ti_5Al_2C_3$
Space group			$R\bar{3}m$ (166)
Lattice parameters (nm)			$a = 0.302$
			$c = 4.890$
Atom positions	Ti_1	(3*a*)	(0, 0, 0)
	Ti_2	(6*c*)	(2/3, 1/3, 0.04)
	Ti_3	(6*c*)	(2/3, 1/3, 0.15)
	Al	(6*c*)	(0, 0, 0.09)
	C_1	(6*c*)	(1/3, 2/3, 0.02)
	C_2	(3*b*)	(0, 0, 0.5)

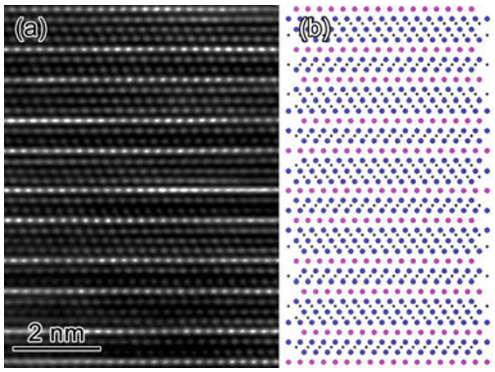

Fig. 5 (a) HRTEM image of $Ti_5Al_2C_3$ taken with the incident beam parallel to the $[11\bar{2}0]$ direction; (b) projection on $(11\bar{2}0)$ plane of $Ti_5Al_2C_3$.

Palmquist *et al.*[4] synthesized $Ti_5Si_2C_3$ in thin film, and constructed a relative stacking sequence of atom layers of Ti, Si, C. According to the constructed stacking sequence, three repetition of alternating three Ti layers and two Ti layers will broke the symmetry of space group D_{6h}^4. Wang *et al*. [8] proposed a crystal structure of the space group $P6_3/mmc$, allowing the edge sharing Ti_6C octahedrons a slight distortion. To compare these two crystal structures, theoretical structure optimizations were conducted using these two types of structure as input models. The calculated total energies are −25818.4489 eV for $Ti_{15}Al_6C_9$ ($R\bar{3}m$) and −17210.0654 eV for $Ti_{10}Al_4C_6$ ($P6_3/mmc$), respectively. The latter crystal structure has a total energy of −25815.0981 eV when its formula is written in $Ti_{15}Al_6C_9$, demonstrating that the crystal structure of the space group $P6_3/mmc$ is less stable. However, the reason why the symmetry of $P6_3/mmc$ is broken and reduced to $R\bar{3}m$ is not clear at present. Moreover,

Table 2 Structure parameters of $Ti_5Al_2C_3$

Formula			$Ti_5Al_2C_3$	
Space group			$R\bar{3}m$ (166)	
Methods			Rietveld refined	*Ab initio* calculation
Lattice parameters (nm)			$a = 0.30564$	$a = 0.30752$
			$c = 4.81846$	$c = 4.85868$
Atom positions	Ti_1	(3*a*)	(0, 0, 0)	(0, 0, 0)
	Ti_2	(6*c*)	(2/3, 1/3, 0.0497)	(2/3, 1/3, 0.0487)
	Ti_3	(6*c*)	(2/3, 1/3, 0.1428)	(2/3, 1/3,0.1431)
	Al	(6*c*)	(0, 0, 0.0960)	(0, 0, 0.0961)
	C_1	(6*c*)	(1/3, 2/3, 0.0275)	(1/3, 2/3, 0.0267)
	C_2	(3*b*)	(0, 0, 0.5)	(0, 0, 0.5)

Raman spectrum of $Ti_5Al_2C_3$ (not shown here) indicates that the symmetry of $R\bar{3}m$ is probably broken in some cases. This issue will be discussed in detail elsewhere. Anyhow, much work is needed to further understand the complex crystal structure of this newly discovered compound, which is in progress.

4 Conclusions

In summary, nanolamilated $Ti_5Al_2C_3$ has been determined to crystallize in the $R\bar{3}m$ space group. The refined lattice parameters are $a = 0.305\ 64$ nm, $c = 4.818\ 46$ nm. Atom positions are determined as Ti_1 at 3*a*(0, 0, 0), Ti_2 at 6*c*(2/3, 1/3, 0.0497), Ti_3 at 6*c*(2/3, 1/3, 0.1428), Al at 6*c*(0, 0 , 0.0960), C_1 at 6*c* (1/3, 2/3, 0.0275), C_2 at 3*b*(0, 0, 0.5).

Acknowledgement

This work was funded by the NSFC under Grant No. 50832008, Grant No. 91226202 and the IMR innovative research foundation.

References

[1] Wang XH, Zhou YC. Layered machinable and electrically conductive Ti_2AlC and Ti_3AlC_2 ceramics: A review. *J Mater Sci Technol* 2010, **26**: 385-416.

[2] Barsoum MW. The $M_{N+1}AX_N$ phases: A new class of solids; thermodynamically stable nanolaminates. *Prog Solid State Chem* 2000, **28**: 201-281.

[3] Eklund P, Beckers M, Jansson U, *et al*. The $M_{n+1}AX_n$ phases: Materials science and thin-film processing. *Thin Solid Films* 2010, **518**: 1851-1878.

[4] Palmquist JP, Li S, Persson POA, *et al*. $M_{n+1}AX_n$ phases in the Ti-Si-C system studied by thin-film synthesis and ab initio calculations. *Phys Rev B* 2004, **70**: 165401.

[5] Högberg H, Eklund P, Emmerlich J, *et al*. Epitaxial Ti_2GeC, Ti_3GeC_2, and Ti_4GeC_3 MAX-phase thin films grown by magnetron sputtering. *J Mater Res* 2005, **20**: 779-782.

[6] Wilhelmsson O, Palmquist JP, Lewin E, *et al*. Deposition and characterization of ternary thin films within the Ti-Al-C system by DC magnetron sputtering. *J Cryst Growth* 2006, **291**: 290-300.

[7] Zhou YC, Meng FL, Zhang J. New MAX-phase compounds in the V-Cr-Al-C system. *J Am Ceram Soc* 2008, **91**: 1357-1360.

[8] Wang XH, Zhang H, Zheng LY, *et al*. $Ti_5Al_2C_3$: A New ternary carbide belonging to MAX phases in the Ti-Al-C system. *J Am Ceram Soc* 2012, **95**: 1508-1510.

[9] Lane N, Naguib M, Lu J, *et al*. Structure of a new bulk $Ti_5Al_2C_3$ MAX phase produced by the topotactic transformation of Ti_2AlC. *J Eur Ceram Soc* 2012, **32**: 3485-3491.

[10] Lane N, Naguib M, Lu J, *et al*. Comment on "$Ti_5Al_2C_3$: A new ternary carbide belonging to MAX phases in the Ti-Al-C system. *J Am Ceram Soc* 2012, **90**: 3352-3354.

[11] Mikhalenko SI, Kuz'ma YB, Popov VE, *et al*. New ternary carbides $ZrAlC_{2-x}$ and $HfAlC_{2-x}$ and their crystal structure. *Inorg Mater* 1979, **15**: 1532-1535.

[12] Schuster JC, Nowotny H. Investigations of the ternary systems (Zr, Hf, Nb, Ta)-Al-C and studies on complex carbides. *Z Metallkd* 1980, **71**: 341-346.

[13] Parthé E, Chabot B. $Zr_2Al_3C_{5-x}$ and $Hf_2Al_3C_{5-x}$ described with higher symmetrical space group $P6_3/mmc$. *Acta Crystallogr* 1988, **44**: C774-C775.

[14] Gesing TM, Jeitschko W. The crystal structures of $Zr_3Al_3C_5$, $ScAl_3C_3$, and UAl_3C_3 and their relation to the structure of $U_2Al_3C_4$ and Al_4C_3. *J Solid State Chem* 1998, **140**: 396-401.

[15] Lin ZJ, Zhuo MJ, He LF, *et al*. Atomic scale microstructures of $Zr_2Al_3C_4$ and $Zr_3Al_3C_5$ ceramics. *Acta Mater* 2006, **54**: 3843-3851.

[16] Wang XH, Zhou YC. Solid-liquid reaction synthesis and simultaneous densification of polycrystalline Ti_2AlC. *Z Metallkd* 2002, **93**: 66-71.

[17] Wang XH, Zhou YC. Solid-liquid reaction synthesis of layered machinable Ti_3AlC_2 ceramic. *J Mater Chem* 2002, **12**: 455-460.

[18] Segall MD, Lindan PJD, Probert MJ, *et al*. First-principles simulation: Ideas, illustrations and the CASTEP code. *J Phys Condens Matter* 2002, **14**: 2717-2744.

[19] Pack JD, Monkhorst HJ. Special points for brillouin-zone integrations: A reply. *Phys Rev B* 1997, **16**: 1748-1749.

[20] Vanderbilt D. Soft self-consistent pseudopotentials in a generalized eigenvalue formalism. *Phys Rev B* 1990, **41**: 7892-7895.

[21] Perdew JP, Chevary JA, Vosko SH, *et al*. Atoms, molecules, solids, and surfaces: Applications of the generalized gradient approximation for exchange and coorelation. *Phys Rev B* 1992, **46**: 6671-6687.

[22] Fischer TH, Almlof J. General methods for geometry and wave function optimization. *J Phys Chem* 1992, **96**: 9768-9774.

[23] Williams DB, Carter CB. *Transmission Electron Microscopy*: *A Textbook for Materials Science*. Beijing (China): Tsinghua University Press, 2007.

[24] Morniroli JP, Steeds JW. Microdiffraction as a tool for crystal structure identification and determination. *Ultramicroscopy* 1992, **45**: 219-239.